

Planar SFS Josephson Junctions Made by Focused Ion Beam Etching.

V.M. Krasnov, O. Ericsson, S. Intiso, and P. Delsing

*Department of Microtechnology and Nanoscience,
Chalmers University of Technology, SE-41296 Gothenburg, Sweden*

V.A. Oboznov, A.S. Prokofiev, and V.V. Ryazanov

Institute of Solid State Physics, Russian Academy of Sciences, 142432 Chernogolovka, Russia

Superconductor-Ferromagnet-Superconductor (S-F-S) Josephson junctions were fabricated by making a narrow cut through a S-F double layer using direct writing by Focused Ion Beam (FIB). Due to a high resolution (spot size smaller than 10 nm) of FIB, junctions with a small separation between superconducting electrodes (≤ 30 nm) can be made. Such a short distance is sufficient for achieving a considerable proximity coupling through a diluted CuNi ferromagnet. We have successfully fabricated and studied S-F-S (Nb-CuNi-Nb) and S-S'-S (Nb-Nb/CuNi-Nb) junctions. Junctions exhibit clear Fraunhofer modulation of the critical current as a function of magnetic field, indicating good uniformity of the cut. By changing the depth of the cut, junctions with the $I_c R_n$ product ranging from 0.5 mV to $\sim 1\mu\text{V}$ were fabricated.

PACS numbers:

INTRODUCTION

Superconducting circuits, containing hybrid Superconductor - Ferromagnet (S-F) structures are of considerable interest for possible applications in cryoelectronics. Exchange interaction in a ferromagnet results in splitting of electron spectra for spin up and - down orientations. Therefore, Cooper pairs, consisting of electrons with opposite spin acquire the momentum $Q = E_{ex}/v_F$, where E_{ex} is the exchange energy in the ferromagnet and v_F is the Fermi velocity, when they penetrate into the ferromagnet via the proximity effect at the S-F interface. This leads to an oscillating superconducting order parameter $\psi \propto \cos(2Qx)$, which in turn could lead to a sign reversal of the order parameter in the S-F-S structure and formation of the π -junction, exhibiting a spontaneous π -shift in the phase difference or the negative Josephson coupling, when the thickness of the F-layer is close to an odd integer number of half the oscillation period [1]. Structures including arrays of conventional 0- and π -junctions can operate as "phase batteries" which can minimize interactions with the dephasing environment and could allow realization of a "quiet" phase qubit- the basic element of a quantum computer [2] or can be used for building complimentary Josephson digital devices [3] and novel modification of Rapid Single Flux Quantum logic [4].

Such S-F-S π -junctions were fabricated recently [5, 6] and existence of a spontaneous π -shift in a triangular SFS-junction array [7] and one-junction interferometers [8] was also demonstrated. However, there are still considerable technical difficulties, which have to be overcome before such junctions could be used in practical devices. One of the difficulties is associated with a short coherence

length in a ferromagnet:

$$\xi_F^{dirty} = \sqrt{\frac{\hbar D}{E_{ex}}}, \quad (1)$$

where D is a diffusion coefficient of electrons in a dirty ferromagnet. For common ferromagnets with $E_{ex} \sim 1000\text{K}$, ξ_F is in the range of a nanometer, as observed, eg., for pure Ni [9, 10]. For the sake of reproducibility, the roughness of such a ferromagnetic film has to be kept at the atomic level. This impose very strong demands on fabrication techniques. To avoid this difficulty, diluted ferromagnetic alloys with a reduced E_{ex} can be employed. Approximately a ten-fold increase of the ferromagnetic coherence length in diluted CuNi[5] and PdNi[6] alloys was achieved, resulting in a successful fabrication of S-F-S π -junctions using conventional thin film deposition techniques. Another technical difficulty is caused by a necessity to fabricate both 0- and π - junctions at the same chip in one run, required for practical quantum device.

In this paper we report a novel fabrication technique for planar S-F-S junctions by Focused Ion Beam (FIB) etching. FIB allows fabrication of nano-scale structures and has a great flexibility, which is important for fabrication of more complicated circuits containing 0 and π -junction arrays. Previously it was demonstrated that FIB can be used for fabrication of proximity-coupled Superconductor-Normal metal-Superconductor (Nb-Cu-Nb) junctions[11] and SQUID's[12]. Here we fabricate Superconductor-Ferromagnet-Superconductor Josephson junctions by making a narrow FIB cut through a S-F double-layer. Due to a high resolution (spot size smaller than 10 nm) of FIB, junctions with a small separation between superconducting electrodes (≤ 30 nm) can be

easily made. Such short distance is sufficient to achieve a considerable proximity coupling through a diluted CuNi ferromagnet. We have successfully fabricated and studied S-F-S (Nb-CuNi-Nb) and S-S'-S (Nb- Nb/CuNi-Nb) junctions. Junctions exhibit clear Fraunhofer modulation of the critical current as a function of magnetic field, indicating good uniformity of the cut. Changing the depth of the cut, junctions with the $I_c R_n$ product ranging from 0.5 mV to $\sim 1\mu V$ were fabricated.

In comparison to fabrication techniques for sandwich (overlap) type S-F-S junctions reported so far[5, 6], our technique for fabrication of planar S-F-S junction using FIB is much simpler and considerably more flexible. This technique can be used for fabrication of 0 or π -junctions and 0 - π -junction SQUIDS in one run by changing the depth and the width of the cut.

SAMPLE FABRICATION

$\text{Cu}_{0.47}\text{Ni}_{0.53}/\text{Nb}$ bilayers were deposited on oxidized Si substrates by RF and DC magnetron sputtering, respectively. The $\text{Cu}_{0.47}\text{Ni}_{0.53}$ alloy had a Curie temperature $\sim 60\text{K}$ and the coherence length $\xi_F \sim 2\text{-}7\text{ nm}$, Eq. (1). The bilayer was patterned by optical lithography and Ar ion milling to define 4-5 μm wide electrodes and contact pads. The sample was then transferred to a standard FIB (FEI Inc. FIB-200) for the junction fabrication. The Ga ion beam had a dwell time of 0.3 μs , a beam spot overlap of 30%, and an acceleration voltage of 30 kV through the process. The top panel in Fig.1 shows a sketch of the fabrication procedure. After focusing and correcting the astigmatism, a single cut through the top Nb layer was made at the beam current of 1 pA. The width of the cut is determined by the FIB spot size ($< 10\text{nm}$). Finally, at the beam current of 10 pA, rectangular patterns at the edges of electrodes were etched to avoid electrical shorts from the material resputtered during Ar ion milling.

The bottom panel in Fig.1 shows a secondary electron image of the junction. The width of the cut at the top of Nb layer is $\sim 30\text{ nm}$. We believe that walls of the cut are not completely vertical and the actual width of the cut at the CuNi layer is narrower (down to the spot size of $\sim 10\text{ nm}$). The depth of the cut was altered by changing the etching time. The etching rates of Nb and CuNi were estimated to be $\sim 10^{-9}\text{m}^3/\text{C}$ by etching $2 \times 2\mu\text{m}^2$ square at the 10 pA beam current and using the end point detection. However, we experienced that the etching rate becomes somewhat smaller for deep cuts with the width-to-depth aspect ratio more than two. Most probably, this is caused by resputtering of material inside the trench, which is also partly responsible for the walls of the cut being non-vertical. To change the aspect ratio of the cut required for a complete etching through the Nb layer, and thus to change the effect of resputtering, we have studied junctions made from two types of Nb/CuNi double layers

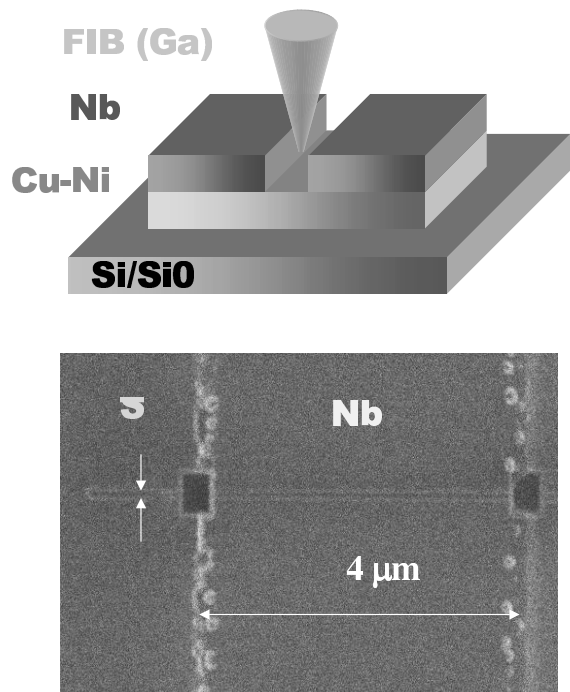


FIG. 1: Top panel: A sketch of the fabrication procedure and the sample geometry. Bottom panel: a secondary electron image of the junction.

with either 70 or 25 nm thick Nb layer. The thickness of the CuNi layer was always 50 nm. Measurements were done in a four probe configuration in a He^4 cryostat or a He^3/He^4 dilution refrigerator.

RESULTS AND DISCUSSION

Fig.2 shows a resistive transition of a Nb(70nm)/CuNi(50nm) junction. The inset shows the overall transition. Here the resistance $\sim 100\Omega$ is predominantly the resistance of the bilayered Nb/CuNi bridge. It is seen that upon cooling down, the resistance of the bridge first drops abruptly at $T_c = 7.5\text{K}$, followed by a relatively broad transition which ends at $\sim 5 - 6\text{K}$. Unlike the transition at T_c , the width of the second transition changes from sample to sample and probably represents a spontaneous flux-flow resistance of the Nb/CuNi bridge[13] caused by stray magnetic fields in the ferromagnetic layer, which depend on a magnetic domain structure of a particular sample. The resistive transition of the junction itself is almost invisible in the inset of Fig.2 and is shown in detail in the main panel of Fig.2. It is seen that the resistance R_n of the junction is much smaller than the resistance of the bridge. For junctions with a measurable critical current, R_n ranges from ~ 0.2 to $\sim 1.0\Omega$, which is comparable with the resistance of $\sim 0.1 - 0.2\Omega$ for our CuNi alloy with the resistivity $\rho \simeq 60\mu\Omega\text{cm}$, the thick-

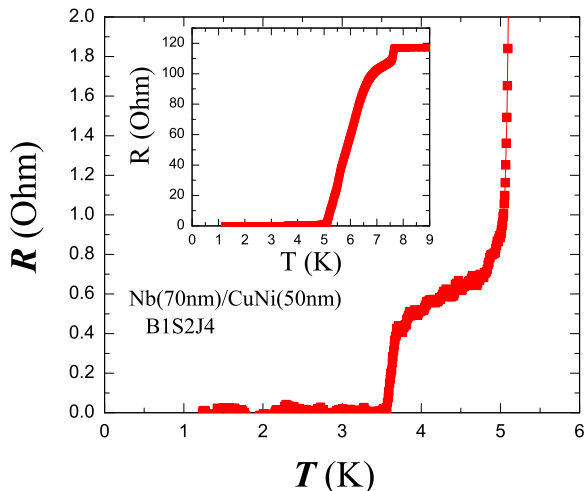


FIG. 2: A typical resistive transition of a Nb(70nm)/CuNi(50nm) junction

ness (the depth of the current path) $\sim 20 - 50nm$, the length $\sim 20 - 30nm$ and the width $\sim 4 - 5\mu m$.

Fig. 3 shows current voltage characteristics (IVC's) of another Nb(70nm)/CuNi(50nm) junction at different base temperatures. Inset shows IVC's at elevated temperatures. It is seen that the onset of the critical current, I_c , is sharp and well defined even at elevated temperatures. At lower temperatures IVC's exhibit a hysteresis, so that the retrapping current, I_r , at which the junction switch from the resistive to the superconducting state is smaller than the critical current, I_c , see the IVC at $T = 1.2K$ in Fig.3. With increasing temperature the hysteresis (the difference between J_c and J_r) vanishes as demonstrated in Fig.4 for two Nb(25nm)/CuNi(50nm) junctions. A similar hysteresis was also reported for Nb/Cu planar junctions and was attributed to the self-heating phenomenon [12]. Indeed, self-heating could be considerable for S-S'-S junctions with large I_c . However, we observed a similar hysteresis even in S-F-S type junctions with the same geometry but with a three order of magnitude smaller I_c and proportionally smaller dissipation power at the retrapping current, P_r . For example, the junction B2S1aJ1 with a large critical current $I_c = 1.58mA$ and the dissipation power $P_r = 37.7nW$ exhibits the hysteresis $I_c/I_r = 2.7$ at $T = 30mK$; the junction B2S1aJ6 with an intermediate $I_c = 175\mu A$ and $P_r = 1nW$ has $I_c/I_r = 2.1$ at $T = 30mK$, see Fig.4; while the junction B2S1aJ5 Nb(25nm)/CuNi(50nm) with a small $I_c = 34.5\mu A$ and $P_r = 73.5pW$ has $I_c/I_r = 1.4$ at $T = 30mK$, i.e., the hysteresis has decreased by less than a factor two despite the decrease of the dissipation power P_r by 513 times. All of those three junctions were fabricated on the same chip, had the same geometry, except for the depth of the cut, and, inevitably, similar thermal conductances, and were measured under

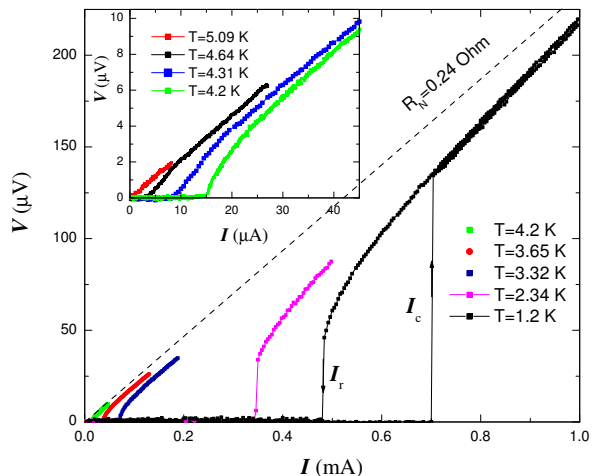


FIG. 3: Current voltage characteristics at different temperatures for a Nb(70nm)/CuNi(50nm) junction.

the same conditions. Therefore, it is unlikely that the self heating alone could explain the observed hysteresis in IVC's. In general, the hysteresis in IVC's at low temperatures is quite a common phenomenon in superconductor-normal metal-superconductor weak links and can also be attributed to non-equilibrium phenomena[14, 15] or frequency dependent damping[16]. Recently a hysteresis in planar superconductor-two dimensional electron gas-superconductor junctions was shown to be dominated by a considerable stray capacitance of electrodes[17].

In Fig.4, temperature dependencies of the linear critical current density J_c (A/m) are shown for Nb(70nm)/CuNi(50nm) and Nb(25nm)/CuNi(50nm) junctions. It is seen that the critical current density can be varied within three orders of magnitude by changing the etching time, i.e. the depth of the cut. For example, if we take the junction B1S1J4 as a reference point (etching time 80 sec. for a $6\mu m$ long line), an increase of etching time by 12.5% (90 sec.) for the junction B1S1J3 leads to a two fold decrease of $J_c(T = 1.2K)$. However, further increase of the etching time by 50% (120 sec) for the junction B1S1J2 leads to a 70-fold drop of $J_c(T = 1.2K)$. Apparently, such a dramatic drop in J_c , which is associated with a small change of the etching time (depth) and a negligible change in the junction resistance, occurs at the threshold of a complete etching through the Nb layer. Therefore, junctions B1S1J4 and B1S1J3 are of S-S'-S (Nb-Nb/CuNi-Nb) type, where the weak link S' consists of a thin underetched Nb layer with suppressed superconducting properties due to proximity effect with the underlying CuNi alloy, while the junction B1S1J2 is of S-F-S (Nb-CuNi-Nb) type. Taking into account the difference in etching times and critical currents between samples B1S1J4 and B1S1J3, and assuming that in B1S1J3 not more than $\xi_s \sim 10nm$ of Nb is left, we can estimate the etching rate to be $\sim 0.36 nm/sec$ per μm of

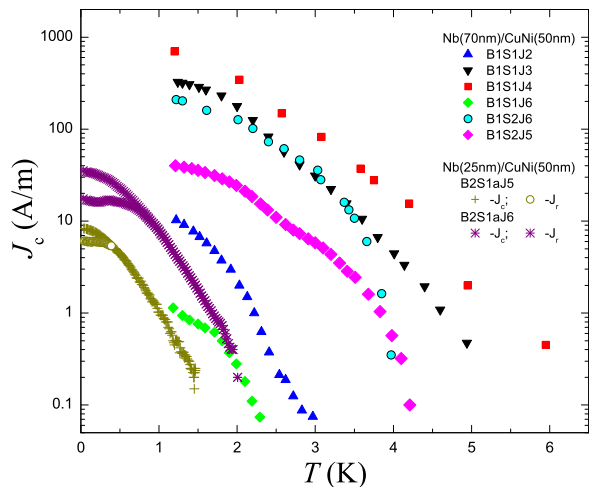


FIG. 4: Temperature dependence of the linear critical current density for junctions with different depth and width of the cut and different thickness of the Nb electrode.

the cut at the FIB current of 1 pA, which is consistent with the measured etching rate of $\sim 10^{-9}m^3/C$, for the width of the cut ~ 30 nm, see Fig.1. Similar estimations for B1S1J2 indicate that for this junction we have etched not more than 5 nm into the CuNi alloy.

The critical current continues to decrease rapidly with increasing the depth of the cut into the CuNi. Here one has to compare the depth of the cut into CuNi with the coherence length $\xi_F \sim 2 - 7nm$. For deeper cuts effective length of the ferromagnetic link in such planar S-F-S junctions becomes longer, causing the rapid decrease of J_c .

In contrast to the critical current, the normal resistance of the junction does not exhibit any peculiarity at the threshold of etching through Nb. For example, the normal resistance increased by merely 30% from junction B1S1J3 ($R_n \simeq 0.26\Omega$) to junction B1S1J2 ($R_n \simeq 0.33\Omega$), which is consistent with estimation of the remaining thickness of the film after cutting. For junctions with a smallest measurable critical current density, $J_c \sim 0.1A/m$, R_n increases to $\sim 1.0\Omega$, i.e., by approximately a factor of five in comparison with the S-S'-S junction B1S1J4, while the critical current decreased more than a thousand times. Since the critical current is much more sensitive to the depth of the cut than the normal resistance, the $I_c R_n$ product decreases with increasing the depth of the cut. For junctions shown in Fig. 4, the $I_c R_n$ ranges from ~ 0.5 mV to $\sim 1\mu V$ at the lowest temperature, with the $I_c R_n$ product at the threshold of cutting through the Nb layer being $\sim 10 - 20\mu V$.

From Fig.4 it is seen that the critical current has a strong temperature dependence (note the logarithmic scale in J_c axis) with a positive curvature of $J_c(T)$ close to T_c . Such behavior is typical for long Superconductor-Normal metal-Superconductor junctions, in which the

length of the normal metal exceeds the coherence length, ξ_N [18]. This is probably the case for our S-S'-S junctions, in which S' can behave as a normal metal due to a strong proximity effect between a thin Nb layer and the underlying CuNi film. However, we also observed a strong $J_c(T)$ dependence for nominally S-F-S junctions, which was unexpected, since for $E_{ex} \simeq 60K$ for our CuNi alloy, the coherence length ξ_F has a negligible temperature dependence in the corresponding temperature range, $\pi kT \ll E_{ex}$. We could suggest that the strong $J_c(T)$ dependence can be due to several reasons: first, if the walls of the cut are not perfectly vertical, the current is flowing from regions with gradually vanishing thickness of Nb, and therefore continuously varying T_c [13]. It can also be caused by the implantation of Ga into Nb and CuNi alloy, by the damage of surface layers of both Nb and CuNi and by resputtering of material inside the cut. All this might lead to local suppression of T_c of Nb and formation of a thin non-magnetic layer at the surface of CuNi alloy. The depth of implantation of Ga into Cu was estimated to be ~ 10 nm [11]. The resputtering can be reduced by decreasing the thickness of Nb and, therefore, the aspect ratio of the cut. As seen from Fig. 4, decreasing of the Nb thickness from 70 to 25 nm does not introduce major changes in the $J_c(T)$ behavior, except for a reduced T_c , which indicates that resputtering is probably not the major reason for the observed strong $J_c(T)$ dependence.

Fig.5 shows a typical dependence of the critical current versus magnetic field, $I_c(H)$, for a S-F-S type Nb(25nm)/CuNi(50nm) junction B2S1aJ6 at $T = 30mK$. Magnetic field was applied perpendicular to the film, as required by the planar structure of the junction, see Fig.1. It is seen that the $I_c(H)$ exhibits clear Fraunhofer oscillations, indicating a good homogeneity of the critical current, and thus homogeneity of the depth and the width of the cut along the length of the junction. The periodicity of Fraunhofer oscillations is about an order of magnitude smaller than $\Delta H = \Phi_0/L\Lambda$, where Φ_0 is the flux quantum, L is the length of the junction, and $\Lambda \simeq 2\lambda + d$ - the effective magnetic width, where λ is the London penetration depth and d is the width of the FIB cut. The discrepancy is due to the fact that in our case magnetic field is applied not parallel, but perpendicular to the superconducting film. In this configuration flux focusing at the edges of the superconducting film takes place and the effective magnetic field, experienced by the junction, is $H_{eff} = H/(1 - D)$, where D is the effective demagnetization factor of the superconducting film[19]. For a thin film in parallel magnetic field $D_{\parallel} \simeq 0$ and flux focusing effect is negligible. However in a perpendicular field $D_{\perp} \simeq 1$ [20], leading to a considerably smaller periodicity of Fraunhofer modulation $\Delta H = \Phi_0(1 - D_{\perp})/L\Lambda$.

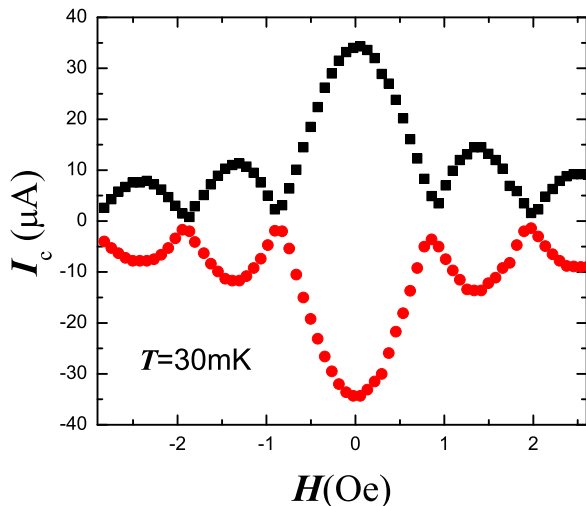


FIG. 5: A Fraunhofer pattern $I_c(H)$ for a Nb(25nm)/CuNi(50nm) junction.

CONCLUSIONS

In conclusion, planar superconductor-ferromagnet-superconductor Josephson junctions were fabricated by direct writing with Focused Ion Beam. Junctions exhibit clear Fraunhofer modulation of the critical current as a function of magnetic field, indicating good uniformity of the FIB cut. By changing the depth of the FIB cut we could fabricate both variable thickness SS'S bridges with $I_c R_n$ up to $0.5mV$, when the cut is stopped within the Nb-layer, and SFS junctions with $I_c R_n$ down to $1\mu V$, when the Nb-layer is completely cut through. The cut through Nb layer is accompanied by a dramatic drop of the critical current density and only marginal change of the junction resistance. Finally we argue that flexibility of FIB allows simultaneous fabrication of "0-" and " π -" junctions in one run, by adjusting the depth of the cut and the width of the junction. Such circuits would be required for future applications of SFS junctions in novel cryoelectronic devices.

ACKNOWLEDGMENTS

The work was supported by INTAS-2001-0809 and Program of Russian Academy of Sciences. We are grateful to T.Bauch for assistance in experiment.

- (1982)]; A. I. Buzdin, B. Vujichich, M. Yu. Kupriyanov, Zh. Eksp. Teor. Fiz. 101, 231 (1992) [Sov. Phys. JETP 74, 124 (1992)]; E.A.Demler, G.B.Arnold and M.R.Beasley, Phys. Rev.B 55 (1997) 15174
- [2] G. Blatter, V. B. Geshkenbein, and L. B. Ioffe, Phys. Rev. B 63 (2001) 174511.
- [3] E. Terzioglu, M.R. Beasley, IEEE Trans. Applied Superconductivity, 8(2), 48-53 (1998).
- [4] A.V.Ustinov, V.K.Kaplunenko. Journ. Appl. Phys. 94, 5405 (2003).
- [5] Veretennikov, V.V.Ryazanov, V.A.Oboznov, A.Yu.Rusanov, V.A.Larkin and J.Aarts., Physica B 284-288 (2000) 495; V.V.Ryazanov, V.A.Oboznov, A.Yu.Rusanov, A.V.Veretennikov, A.A.Golubov and J.Aarts, Phys. Rev. Lett. 86, 2427 (2001);
- [6] T. Kontos, M. Aprili, J. Lesueur, and X. Grison, Phys. Rev. Lett. 86 (2001) 304; T.Kontos, M.Aprili, J.Lesueur, F.Genet, B.Stephanidis and R.Boursier, ibid. 89 (2002) 137007
- [7] V.V.Ryazanov, V.A.Oboznov, A.V.Veretennikov and A.Yu.Rusanov Phys.Rev. B 65 (2002) 020501(R)
- [8] S.M.Frolov, D.J. Van Harlingen, V.A.Oboznov, V.V.Bolginov, and V.V.Ryazanov. arXiv:cond-mat/0402434 (2004), to be published in Phys. Rev. B.
- [9] Y.Blum, A.Tsukernik, M.Karpovski and A.Palevski, Phys.Rev.Lett. 89 (2002) 187004
- [10] J.E.Villegas, E.Navarro, D.Jaque, E.M.Gonzalez, J.I.Martin and J.L.Vicent, Physica C (2002) 213-216
- [11] R.W.Moseley, W.E.Booij, E.J.Tarte, and M.G.Blamire, Appl.Phys.Lett. 75 (1999) 262
- [12] G.Burnell, E.J.Tarte, D.-J. Kang, R.H.Hadfield, and M.G.Blamire, Physica C241-245 (2002) 241
- [13] V.V.Ryazanov, V.A.Oboznov, A.S.Prokof'ev and S.V.Dubonos, JETP Lett. 77 (2003) 39
- [14] Y.Song. Journ. Appl. Phys. 47, 2651 (1976)
- [15] M.Tinkham, Introduction to Superconductivity (McGraw-Hill, 1996)
- [16] R.L.Kautz and J.M.Martinis, Phys.Rev.B 42 (1990) 9903
- [17] S.Intiso, "Fabrication and characterisation of an in-situ capacitively shunted S-2DEG-S field effect transistor", M.Sc thesis Chalmers University of Technology, Gothenburg (2003)
- [18] V.M.Krasnov, Physica C 252 (1995) 319; A.A.Golubov, V.M.Krasnov and M.Yu.Kupriyanov, J. Low Temp.Phys. 106 (1997) 249
- [19] V.M.Krasnov, V.A.Larkin and V.V.Ryazanov, Physica C 174 (1991) 440; V.M.Krasnov and V.V.Ryazanov, ibid. 297 (1998) 153
- [20] L.D.Landau and E.M.Lifshitz, Electrodynamics of Continuous Media (Pergamon, Oxford, 1984), Sec. 4.

[1] A. I. Buzdin, L. N. Bulaevskij, S. V. Panyukov, *Pis'ma Zh. Eksp. Teor.Fiz.* **35** 147 (1982) [JETP Lett. 35, 178